



# Electrochemical behavior of methylene blue at bare and DNA-modified silver solid amalgam electrodes

Veronika Svitková<sup>1</sup> · Vlastimil Vyskočil<sup>2</sup>

Received: 3 November 2021 / Revised: 8 August 2022 / Accepted: 8 August 2022 / Published online: 15 August 2022  
© The Author(s), under exclusive licence to Springer-Verlag GmbH Germany, part of Springer Nature 2022

## Abstract

Cyclic voltammetry (CV) and differential pulse voltammetry (DPV) were used for a voltammetric study of methylene blue (MB) at a mercury meniscus-modified silver solid amalgam electrode (m-AgSAE). Electrochemical impedance spectroscopy (EIS) was used for the verification and comparison of results. DPV offered sensitive detection of MB (in 0.1 mol L<sup>-1</sup> phosphate buffer of pH 7.0) at both a bare and a DNA-modified silver amalgam electrode. MB gives a specific cathodic signal related to the reduction of this redox intercalator. This signal is significantly higher at the DNA-modified than at the unmodified silver amalgam electrode, which is in correspondence with the changes in charge transfer resistance values obtained from Nyquist plots. The concentration of double-stranded DNA (dsDNA) to form a layer (0.1 mg mL<sup>-1</sup>), the time of the dsDNA spontaneous immobilization on the surface of the electrode (1 min), the concentration of MB (1 × 10<sup>-5</sup> mol L<sup>-1</sup>), and the time of the accumulation of MB into the dsDNA layer (1 min) were optimized for further biosensor development and applications.

**Keywords** Silver amalgam electrode · Methylene blue · DNA · Electrochemistry

## Introduction

The electrochemical behavior of methylene blue (MB) and its leucoform — leucomethylene blue (LMB) — in aqueous solutions at pH 7.9 was investigated already in 1981 by Papeschi et al. [1] at a mercury dropping electrode, where the results were compared to those found and published by Brdička in 1942 [2]. In physiological conditions (at laboratory temperature, pH of the environment around 7, and atmospheric oxygen concentration), MB is electrochemically reduced in LMB, and the process involves two electrons and one hydrogen cation [3]. MB is an appropriate candidate to study the partial electrode reaction mechanism and the non-specific surficial interactions in the monolayer of this redox-active molecule formed at the electrode surface. Moreover,

this organic dye has a high affinity with the sugar-phosphate backbone of DNA and has a very clear reduction signal at the electrochemical detection, which makes MB one of the first choices as an indicator for the construction of electrochemical DNA sensors [4]. In some earliest electrochemical experiments, the reduction of MB at a DNA monolayer was attributed to a DNA-mediated process, as the surface is inaccessible to the molecule [5]. The observable electrochemical reduction of MB at a DNA-modified electrode demonstrates that DNA-mediated charge transfer could be used as a sensitive tool for probing nucleic acid structure and base stacking [6]. It is assumed that MB, owing to its planar structure, binds to DNA by an intercalation mechanism [7, 8], although some previous electrochemical studies of MB and its derivatives with DNA revealed that electrostatic binding is also possible. This is because MB should intercalate into DNA when the ionic strength of the solution is low, while as the salt concentration increases, MB binds externally to the DNA simultaneously with intercalation [9, 10]. Based on a detailed energetic analysis of modeled MB complexes, it has been found that MB preferentially binds to the minor groove on A-T alternating DNA, whereas the symmetric intercalation complex is most stable in binding to G-C alternating DNA [11].

✉ Vlastimil Vyskočil  
vlastimil.vyskocil@natur.cuni.cz

<sup>1</sup> Institute of Analytical Chemistry, Faculty of Chemical and Food Technology, Slovak University of Technology in Bratislava, 81237 Bratislava, Slovakia

<sup>2</sup> Department of Analytical Chemistry, Faculty of Science, UNESCO Laboratory of Environmental Electrochemistry, Charles University, 12843 Prague 2, Czech Republic

Silver amalgam electrodes are nowadays suitable alternatives to a hanging mercury drop electrode (HMDE), because these electrodes not only show similar electroanalytical sensitivity and properties but also negligible toxicity and simple manipulation as they can be used multiple times and can easily be miniaturized [12]. The main advantages of silver amalgam electrodes are a wide range of working potentials, simple regeneration of the electrode surface, rapid pre-treatment procedure, long-term activity without significant changes in their sensitivity, mechanical stability, simple preparation in different sizes and shapes, and low toxicity, enabling their use in mobile laboratories and for measurements in flowing systems (HPLC, FIA, etc.) [13–16]. The UNESCO Laboratory of Environmental Electrochemistry in Prague, Czech Republic, has paid over the last 20 years the unflagging attention to the utilization of different types of silver amalgam electrodes as an alternative to mercury electrodes [17, 18].

The silver solid amalgam electrodes (AgSAEs) were prepared using a drawn-out glass tube, whose tip was packed with a fine silver powder, amalgamated by liquid mercury, and connected to an electric contact [19]. The surface of the silver solid amalgam electrode can be mechanically polished by using water suspension of alumina to provide a polished silver solid amalgam electrode (p-AgSAE) [20]. For analytical purposes, a mercury meniscus-modified silver solid amalgam electrode (m-AgSAE) is more suitable, because it provides lower noise and better repeatability of the electrochemical response. This electrode can be prepared by immersing the p-AgSAE surface into a small volume of liquid mercury for 15 s while stirring [21]. Furthermore, the solid amalgam electrode fabricated with silver nanoparticles may be seen as an effective and green tool for electrochemical analysis [22]. Other types of silver amalgam electrodes, such as silver amalgam paste electrodes, silver solid amalgam paste electrodes with an organic pasting liquid, silver solid amalgam composite electrodes, or single crystal silver amalgam microelectrodes, also represent interesting possibilities and alternatives [21]. These electrodes were used for voltammetric and amperometric determinations of various biologically active organic compounds [23–25]. Solid amalgam electrodes also appear to be the promising tools for DNA electrochemistry and biosensor development [26–28].

The main purpose of this work was to study an electrochemical behavior of MB, as a representative of DNA intercalators, at the m-AgSAE. This study should provide a relatively fundamental approach in the field of silver solid amalgam electrodes, on which the DNA is immobilized very well spontaneously without any previous electrode surface modification. The aim was to develop a sensitive and fast method and biosensor construction for the indirect detection of the presence of native double-stranded DNA (dsDNA) on the AgSAE surface. The presence of dsDNA

on DNA-modified AgSAEs has so far been monitored directly only using underdeveloped voltammetric peaks CA (cathodic peak resulting from reduction of cytosine and adenine moieties) and G (anodic peak resulting from previously electrochemically reduced guanine moieties) [29, 30]. To the best of our knowledge, no other published papers — apart from our recently published paper [31] — have paid attention to the detection of the presence of DNA on the AgSAE surface using MB as a redox indicator, which may be used for the further indirect detection of DNA damage by various chemical (drugs, pesticides, etc.) or physical (UV radiation) factors.

## Experimental

### Reagents

The stock solution of MB ( $c = 1 \times 10^{-3} \text{ mol L}^{-1}$ ) was prepared by dissolving an accurately weighed amount of dye in deionized water and stored in the fridge at 4 °C. The stability of the MB solution was monitored by measuring the absorbance by using UV–vis spectrometer. Spectrophotometric study demonstrated that this solution was stable for at least 3 months. Working solutions of MB were prepared freshly before every use. The Britton–Robinson (BR) buffers, containing an equal mixture of 0.04 mol L<sup>-1</sup> acetic acid, boric acid, and phosphoric acid adjusted by 0.2 mol L<sup>-1</sup> sodium hydroxide (of pH range from 2.0 to 12.0), and 0.1 mol L<sup>-1</sup> phosphate buffer (PB, pH 7.0) were used as supporting electrolytes. A 0.2 mol L<sup>-1</sup> potassium chloride solution (KCl) was used for the activation of working electrode surface. A stock solution of salmon sperm double-stranded DNA (Sigma-Aldrich, Germany) was prepared in the PB of pH 7.0 and stored in the fridge. Deionized water produced by a Milli-Q Plus System (Millipore, USA) was used to prepare all solutions. All reagents were of p.a. purity grade and stored in glass vessels at ambient temperature, unless stated otherwise.

### Apparatus

All voltammetric measurements were carried out with an Autolab potentiostat controlled by the NOVA 1.11 software (Metrohm Autolab, Switzerland) using a three-electrode system with an Ag|AgCl (sat. KCl) reference electrode, a platinum wire auxiliary electrode, and a silver solid amalgam working electrode (AgSAE), all arranged in an electrochemical cell with a volume of 10 mL used at ambient temperature. The pH measurements were carried out with a digital pH meter Jenway 4330 (Jenway, UK) with a combined glass electrode (type 924 005). UV–vis spectra were measured using a spectrometer Agilent 8453 (Agilent Technologies, USA) driven by the UV–Visible ChemStation 9.01

software. Measurements were carried out in quartz cuvettes of 1 cm optical path length.

## Procedures

The m-AgSAE was prepared by immersing the surface of a p-AgSAE (polished with alumina powder, 1.1  $\mu\text{m}$ ) into liquid mercury for 15 s while stirring and then rinsed with deionized water. After creating a new meniscus and each day before starting measurements, the working electrode was activated electrochemically in the 0.2 mol L<sup>-1</sup> KCl at -2200 mV for 300 s. Then, an electrochemical regeneration of the working electrode based on 150 times switching the electrode potential between an initial ( $E_{1\text{reg}}$ ) and final ( $E_{2\text{reg}}$ ) regeneration potential for 0.05 s took place. The DNA-modified m-AgSAE was prepared by dipping its surface into DNA solution in PB for 1 min under stirring. Thus-prepared sensor was washed with deionized water and then used. Before starting measurements, oxygen was removed from the measured solution by purging with nitrogen for 60 s. Before entering a voltammetric cell, nitrogen passed through pre-bubbler containing deionized water.

For cyclic voltammetry (CV), the step potential of 3 mV and the scan rate of 20 mV s<sup>-1</sup> were used. For differential pulse voltammetry (DPV), the modulation amplitude of 50 mV, the modulation time of 100 ms, the interval time of 150 ms, the step potential of 3 mV, and the scan rate of 20 mV s<sup>-1</sup> were used. The peak heights recorded using DPV were evaluated from the straight lines connecting the minima before and after the peak. For electrochemical impedance spectroscopy (EIS), the polarization potential of -200 mV, the frequency range from 0.1 to 5000 Hz (51 frequency steps), and the amplitude of 10 mV were used. All curves were measured three times ( $n=3$ ). The parameters of all mathematical and statistical quantities (for a significance level of 0.05) were calculated using an Origin Pro 9.0 software.

## Results and discussion

### Voltammetric behavior of methylene blue at bare silver amalgam electrode

The electrochemical behavior of MB was investigated by means of CV (Fig. 1a) and DPV (Fig. 1c) at the m-AgSAE. At first, the influence of the pH on  $1 \times 10^{-4}$  mol L<sup>-1</sup> MB at the bare m-AgSAE was investigated in the BR buffer with pH values from 2.0 to 12.0. In the negative potential region, MB gave one well-developed cathodic voltammetric peak over the whole pH region. The cathodic peak potentials ( $E_p$ ) were shifted towards more negative values with the pH increasing over the whole pH region. The

$E_p$  vs. pH dependences can be fitted to a linear function in the pH range from 2.0 to 6.0 (number of experimental points 5) and in the pH range from 6.0 to 12.0 (number of experimental points 7), for both CV and DPV.

In the case of CV (Fig. 1b), the cathodic peak potential varied with the pH according to the relationship:

$$E_p(\text{V}) = 0.273 - 0.0763 \times \text{pH} \quad (r^2 = 0.998) \quad (1)$$

*for the pH range from 2.0 to 6.0*

$$E_p(\text{V}) = -0.003 - 0.0290 \times \text{pH} \quad (r^2 = 0.996) \quad (2)$$

*for the pH range from 6.0 to 12.0*

In acidic medium (pH range from 2.0 to 6.0), the absolute value of the slope (in Eq. 1) is closer to the theoretical value 59 mV per pH unit, and, thus, two hydrogen cations and two electrons are expected to be involved in the reduction reaction. The CV peak potential difference ( $\Delta E_p$ ) between the MB reduction peak and oxidation counterpeak in this region is around 30 mV (expected for the two-electron reversible electrode process), and their peak height ratio around one confirms the tendency of this process to reversibility. Scheme 1 shows the reduction mechanism of MB electrode conversion which is widely described in the literature [32–36], involving two electrons and only one hydrogen cation. Thus, the result described above is probably related to protonation of the MB molecule in an environment exhibiting a higher concentration of hydrogen cations [33, 34].

In neutral and alkaline media, the situation is rather more complex, and more peaks appeared at the CV recordings. The first well-developed cathodic peak in neutral and alkaline media (pH values from 6.0 to 12.0) is corresponding to the two-electron reversible reduction of MB to LMB (Scheme 1), while the presence of the second less developed peak observable at more negative potentials indicates the two-electron reduction of the MB molecules which, after having reached the surface of the m-AgSAE by diffusion, are adsorbed at the top of the adsorbed monolayer of MBL in direct contact with the electrode and remain in this adsorbed state after reduction [35]. The absolute value of the slope (in Eq. 2) is close to 30 mV, and the peak potential difference  $\Delta E_p$  in this region is around 50 mV (completely in agreement with the results previously reported on mercury electrodes [33]). Therefore, one hydrogen cation and two electrons are taking part in the reduction reaction, which is in correspondence with the literature [3, 36], when two successive one-electron transfers take place with a fast proton transfer interposed between them, according to Scheme 1 [32].

In the case of DPV (Fig. 1d), the cathodic peak potential varied with the pH according to the relationship:

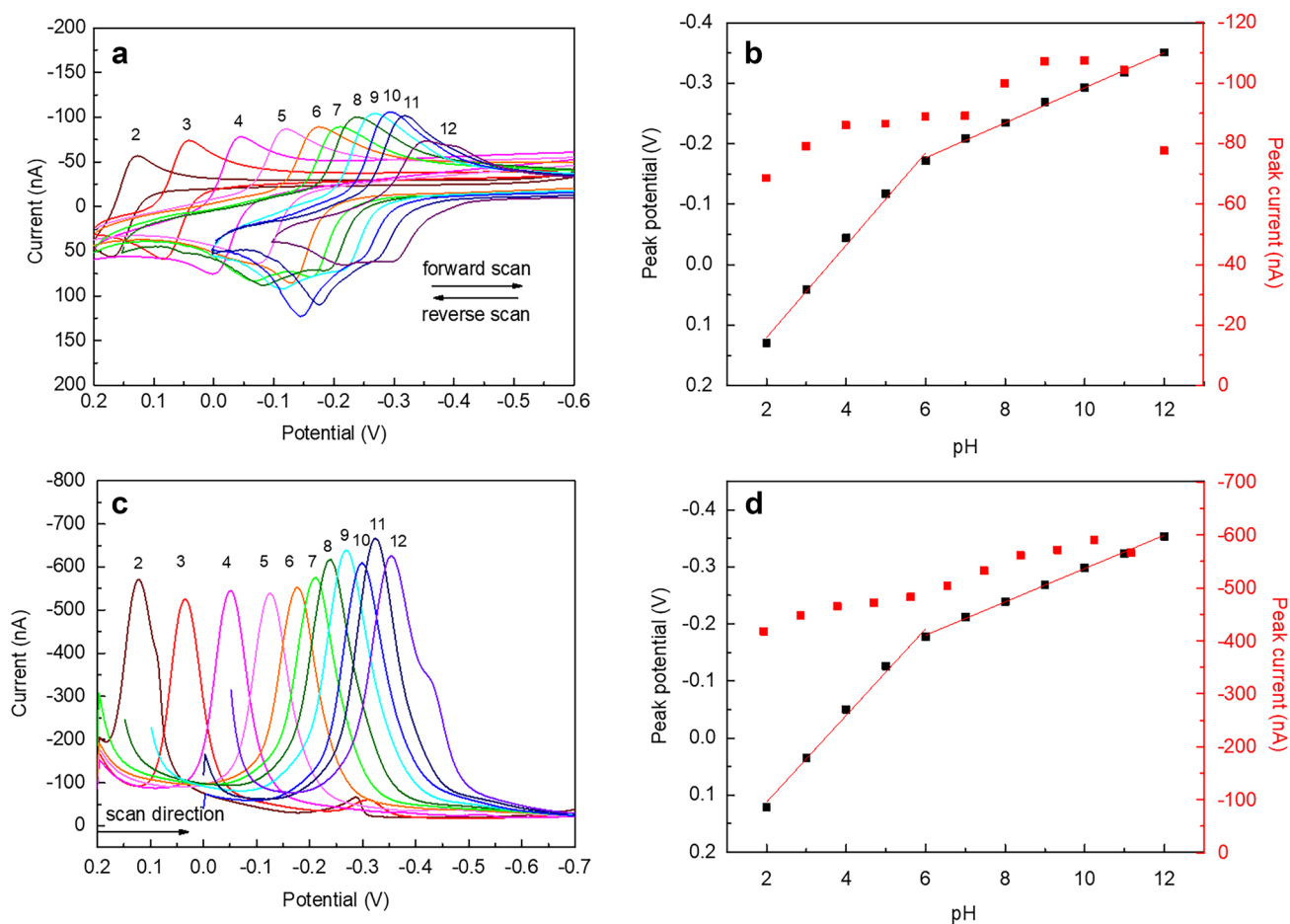
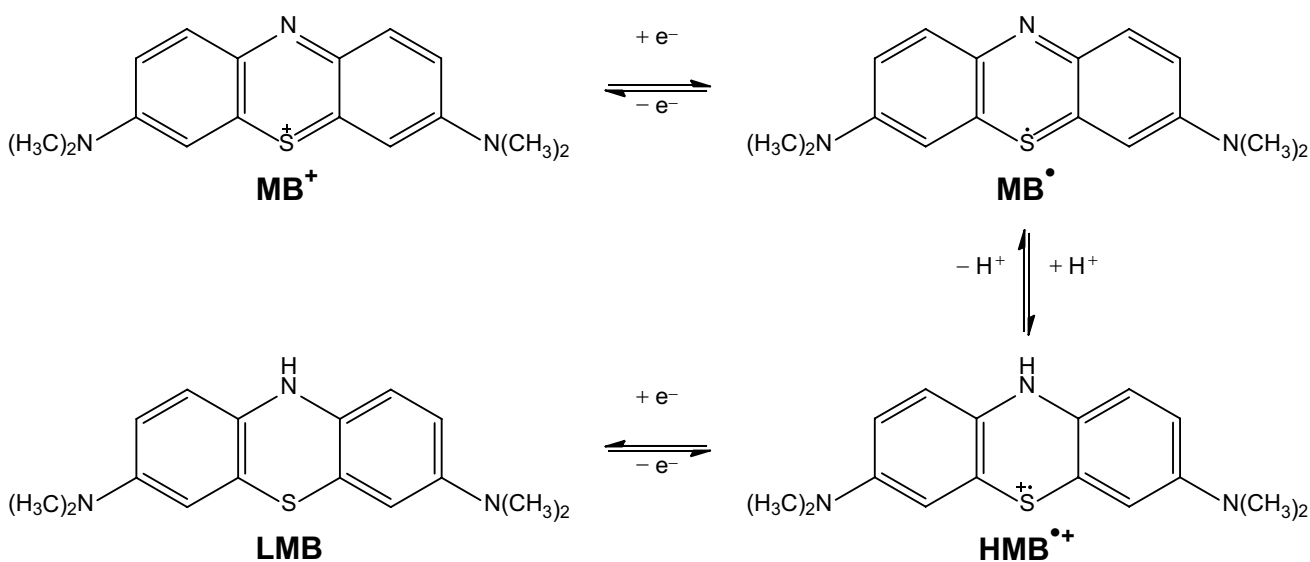


**Fig. 1** CV (a) and DP voltammograms (c) of MB ( $c=1 \times 10^{-4}$  mol  $L^{-1}$ ) recorded at the m-AgSAE in cathodic/anodic (a) and cathodic (c) scans in the BR buffer medium of pH from 2.0 to 12.0. Attached corresponding dependences of CV (b) and DPV (d) peak

potentials (black points) and peak currents (red points) on the resulting pH of the BR buffer medium; the peak potential vs. pH dependences are fitted to a linear function in the pH range from 2.0 to 6.0 and from 6.0 to 12.0 (for corresponding equations, see the text)



**Scheme 1** Reduction mechanism of MB; LMB is leucomethylene blue, and  $HMB^{\bullet+}$  is an intermediate radical cation [32]

$$E_p(\text{V}) = 0.264 - 0.0760 \times \text{pH} \quad (r^2 = 0.989) \quad (3)$$

for the pH range from 2.0 to 6.0

$$E_p(\text{V}) = -0.005 - 0.0292 \times \text{pH} \quad (r^2 = 0.999) \quad (4)$$

for the pH range from 6.0 to 12.0

The dependence of the cathodic peak height ( $I_p$ ) of MB varied with pH over the whole pH region, but these changes were not so significant.

The BR buffer of pH 7.0 was further used for the determination of the analyte in the negative potential region, with the respect to the further DNA–MB host–guest interaction study at a silver amalgam electrode. This is the most frequently used pH value of the supporting electrolyte that is used in the application of DNA-based biosensors and mimics the pH value of a healthy human environment.

Repeated measurements can cause a passivation of the electrode surface resulting in a change of the peak heights and in a shift in the peak potentials. Therefore, appropriate regeneration steps were sought. The repeatability of the DP voltammetric  $I_p$  of  $1 \times 10^{-4}$  mol L<sup>-1</sup> MB in the BR buffer of pH 7.0 was tested. Various combinations of regeneration potentials, together with values obtained without any regenerating treatment (1 min purging of the solution), are shown in Fig. 2. Although Barek with co-workers [23] suggested a series of suitable potential cleaning pulses as the solution of the passivation problem, in this case, simple purging of the working solution with nitrogen took place in order to overcome a passivation of the electrode surface.

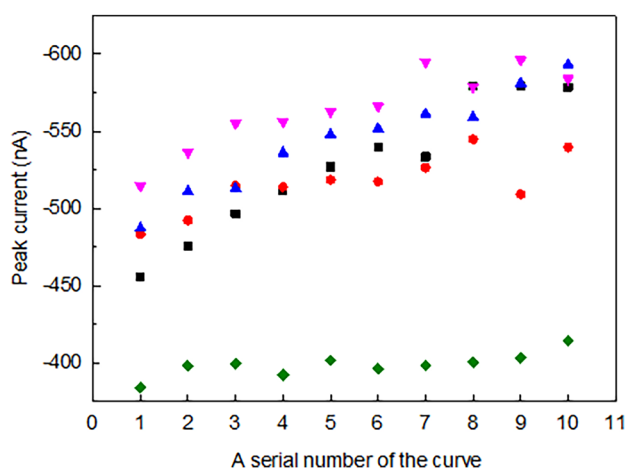


**Fig. 2** The dependence of the peak height of MB ( $c = 1 \times 10^{-4}$  mol L<sup>-1</sup>) in the BR buffer of pH 7.0 on a serial number of successive measurements with an application of different regeneration potentials at the m-AgSAE. The combinations of regeneration potentials were the following: 0, -500 mV (pink triangle); 0, -1200 mV (blue triangle); 200, -1200 mV (black square); 200, -500 mV (red circle); and without regeneration/purging applied (green diamond)

The optimal conditions were used for measuring the concentration dependence (Fig. 3) in the concentration range of MB (in the BR buffer of pH 7.0) from  $1 \times 10^{-7}$  mol L<sup>-1</sup> to  $1 \times 10^{-5}$  mol L<sup>-1</sup> using CV (Fig. 3a) and DPV (Fig. 3b). As can be seen from the DP voltammograms, a “second peak” shifted to more negative potential appears at higher concentrations of MB. This corresponds to the reduction of unadsorbed MB to adsorbed LMB, the extent of this step being limited not only by the diffusion of MB but also by the surface available for adsorption of the reduced molecules [1]. The sensitivity slightly differs over the whole concentration range. Within the particular concentration range (from  $1 \times 10^{-6}$  mol L<sup>-1</sup> to  $1 \times 10^{-5}$  mol L<sup>-1</sup>), the concentration dependence is linear (Fig. 3c), with the corresponding equation:

$$I_p(\text{nA}) = -18.2 - 12.8 \times c(\mu\text{mol L}^{-1}) \quad (r^2 = 0.996) \quad (5)$$

This is related to the adsorption of the MB on the electrode surface. However, in the lower concentration range from  $1 \times 10^{-7}$  mol L<sup>-1</sup> to  $1 \times 10^{-6}$  mol L<sup>-1</sup>, nonlinear regression could be used to fit this dependence. Polynomial regression of the second degree was used for this purpose (Fig. 3d), with the corresponding equation:

$$I_p(\text{nA}) = -1.16 - 55.3 \times c(\mu\text{mol L}^{-1}) + 25.6 \times c^2(\mu\text{mol}^2 \text{L}^{-2}) \quad (r^2 = 0.978) \quad (6)$$

### Voltammetric behavior of methylene blue at DNA-modified silver amalgam electrode

Several types of binding modes, including electrostatic interactions with the negatively charged nucleic sugar-phosphate structure, covalent binding (formation of DNA adducts), and intercalations between the stacked base pairs of dsDNA, take place between small molecules and double-stranded DNA [37]. The binding properties depend on the nature of small molecules and the experimental conditions (e.g., ionic strength, concentration, and pH) [38]. MB is a commonly used DNA intercalator and shows different electrochemical responses on unmodified and DNA-modified electrodes [39].

Electrochemical behavior of MB at the DNA-modified silver amalgam electrode was investigated by means of DPV. DPV (Fig. 4a) was carried out at the DNA/m-AgSAE sensor in the solution of MB in the PB of pH 7.0 to monitor the changes in the intensity of the MB reduction signal. It has been reported that the reduction potential of intercalated MB is cathodically shifted in aqueous solution [40]. The sensor was incubated for various times (the incubation lasting for 1 min, 5 min, and 10 min) was performed in stirred solutions containing  $1 \times 10^{-5}$  mol L<sup>-1</sup> and  $1 \times 10^{-4}$  mol L<sup>-1</sup> MB in the PB) or at various concentrations of DNA in the PB.

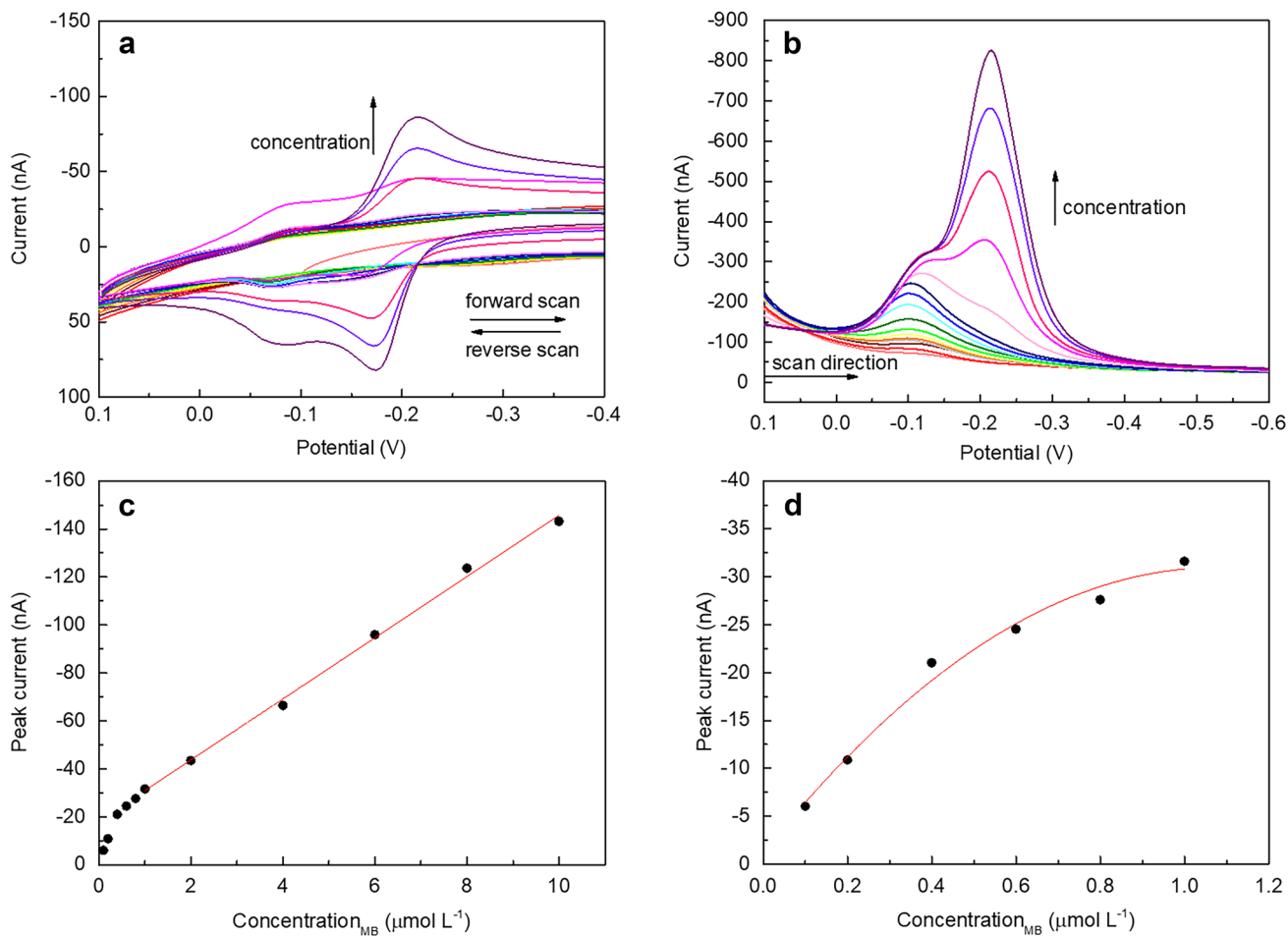


**Fig. 3** CV (a) and DP voltammograms (b) of MB recorded at the m-AgSAE in cathodic/anodic (a) and cathodic (b) scans in the BR buffer of pH 7.0; concentration range of MB from  $1 \times 10^{-7}$  mol L<sup>-1</sup> to

$1 \times 10^{-4}$  mol L<sup>-1</sup>. The peak current vs. concentration dependence corresponding to the DP voltammograms is fitted to a linear function (c) and polynomial function (d)

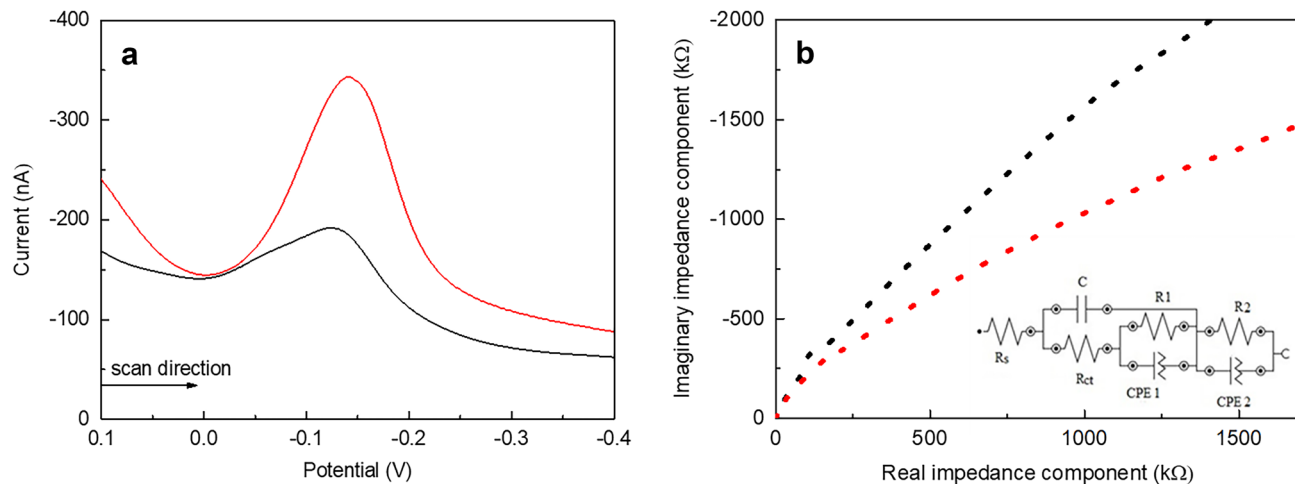


**Fig. 4** DP voltammograms (cathodic scan) (a) and Nyquist plots from EIS (b) of MB ( $c = 1 \times 10^{-5}$  mol L<sup>-1</sup>) recorded at the bare (black) and DNA-modified m-AgSAE (red) in the PB of pH 7.0. Inset of b: corresponding equivalent circuit used for fitting the EIS data

DNA of three different concentrations ( $c_{\text{DNA}} = 0.1 \text{ mg mL}^{-1}$ ,  $1.0 \text{ mg mL}^{-1}$ , and  $10 \text{ mg mL}^{-1}$ ) was adsorbed on the surface of the working electrode. The concentration and incubation time of DNA did not affect the changes of the studied parameters ( $E_p$  and  $I_p$ ). On the other side, the concentration and incubation time of MB have significant effects on the  $I_p$  changes. Therefore, the concentration of DNA of  $0.1 \text{ mg mL}^{-1}$ , the incubation time of 1 min, and the concentration of MB of  $1 \times 10^{-5} \text{ mol L}^{-1}$  were selected as optimum for the preparation of the DNA-based sensor used to obtain the results recently published in our paper [31].

### Electrochemical impedance spectroscopy

The charge transfer resistance of the DNA-modified m-AgSAE in the presence of MB in the PB of pH 7.0 was probed at  $-200 \text{ mV}$  by EIS measurements. The comparison of the Nyquist plots of the EIS spectra is presented in Fig. 4b while a modified Randle's equivalent circuit was used for fitting the EIS spectra (see the inset in Fig. 4b). In the modified Randle's circuit,  $R_s$  simulates the ohmic resistance, and  $R_{ct}$  represents the charge transfer resistance of the electrode–electrolyte interface. The element  $C$  represents capacitance of double electric layer which is charged simultaneously with the occurring electrochemical reaction. The presence of an adsorption complex plays a fundamental role in the deposition of a simpler system [41]. Thus, these experimental data are adequately described by an equivalent electric circuit characteristic of the processes that include the adsorption of an intermediate compound. The double layer capacity and the adsorption capacity are replaced by the respective constant phase elements (CPEs). Consequently, in the Nyquist plot, the semicircle becomes flattened and exhibits the ideal profile of purely diffusion-controlled reaction with almost a linear correlation at lower frequency region [42]. The impedance of the m-AgSAE appeared almost as a linear line, which also indicated excellent conductivity, good electrocatalytic activity, and seamless electron transport on the m-AgSAE–electrolyte interface [43]. The resistance of the electron transfer is significantly lower at the DNA/m-AgSAE (red line) compared to the unmodified electrode (black line). This can be in correspondence with the fact that MB is intercalated into the base pairs of dsDNA, and DNA film serves here as a bridge for charge transport.

### Conclusions

Several strategies have been employed to study the interaction between DNA and MB, and lots of them required chemically modified DNA sequences, e.g., thiol or amine modifications, highly specialized equipment, and, in general, high adsorption times [44]. In the case of silver amalgam

electrodes, there is no need for further modification of the electrode surface or higher times of the adsorption. At the DNA-modified electrode, response of MB was obtained which results in a slight shift of MB peak to lower potential values and a significant increase of this peak, which can be described as the intercalation of the indicator into dsDNA. These data showed that the observed electrochemistry is most efficient at DNA-modified electrodes when the redox probe is bound to the DNA attached at the electrode surface. The previous electrode surface passivation studies showed that in the case of intercalating MB, the DNA base pairs attached at the electrode surface provide a bridge for charge transport. Consequently, surface passivation has no significant effect on the electrochemistry of MB. Any electrochemical processes are observable because MB was employed as a reporter of DNA-mediated processes, since the surface is inaccessible to the molecule. In comparison, the impedance spectra in Nyquist plots exhibited the ideal profile of purely diffusion-controlled reaction with almost a linear correlation at lower frequency region. This also indicated excellent conductivity and lower charge transfer resistance (electron transport) on the m-AgSAE–electrolyte interface. This type of electrode material opens the door to the development of biosensors to detect intercalative processes with a simple, reproducible, and fast methodology. When the electroactive compound, such as MB, is added to the measured system and interacting with DNA noncovalently (via intercalation), the change in the indicator response indicates the change in the DNA structure — strand breaks or helix destruction [31, 45].

**Acknowledgements** VS thanks the Scientific Grant Agency VEGA of the Slovak Republic (Project No. 1/0159/20) and VV thanks the Czech Science Foundation (Project GACR No. 20-01589S) for the financial support of this research. VS, moreover, thanks the Erasmus+ Program of the Slovak Republic for supporting her research stay at the Charles University in Prague. Technical, material, and intellectual support from Metrohm Czech Republic is also gratefully acknowledged.

### Declarations

**Conflict of interest** The authors report no conflicts of interest. The authors alone are responsible for the content and writing of the paper.

### References

1. Papeschi G, Costa M, Bordi S (1981) Electrochemical behavior of methylene blue and its leucoform at the mercury electrode. *Electrochim Acta* 26:1518–1521. <https://doi.org/10.1149/1.2127673>
2. Brdička R (1942) Über die Adsorption des reduzierten Methylenblaus and der tropfenden Quecksilberelektrode. *Z Elektrochem* 48:278–288
3. Barou E, Bouvet M, Heintz O, Meunier-Prest R (2012) Electrochemistry of methylene blue at an alkanethiol modified electrode. *Electrochim Acta* 75:387–392. <https://doi.org/10.1016/j.electacta.2012.05.017>

4. Hua H, Liu Y, Guan X, Li Y (2018) DNA nanosensors based on the use of single gold nanowire electrodes and methylene blue as an intercalator. *Microchim Acta* 185:152. <https://doi.org/10.1007/s00604-018-2703-z>
5. Gorodetsky AA, Buzzeo MC, Barton JK (2009) DNA-mediated electrochemistry. *Bioconjug Chem* 19:2285–2296. <https://doi.org/10.1021/bc8003149>
6. Paleček E, Bartošík M (2012) Electrochemistry of nucleic acids. *Chem Rev* 112:3427–3481. <https://doi.org/10.1021/cr200303p>
7. Kelley SO, Barton JK, Jackson NM, Hill MG (1997) Electrochemistry of methylene blue bound to a DNA-modified electrode. *Bioconjug Chem* 8:31–37. <https://doi.org/10.1021/bc960070o>
8. Yau HCM, Chan HL, Yang M (2003) Electrochemical properties of DNA-intercalating doxorubicin and methylene blue on n-hexadecyl mercaptan-doped 5'-thiol-labeled DNA-modified gold electrodes. *Biosens Bioelectron* 18:873–879. [https://doi.org/10.1016/S0956-5663\(02\)00161-6](https://doi.org/10.1016/S0956-5663(02)00161-6)
9. Vardevanyan PO, Antonyan AP, Parsadanyan MA et al (2013) Mechanisms for binding between methylene blue and DNA. *J Appl Spectrosc* 80:595–599. <https://doi.org/10.1007/s10812-013-9811-7>
10. Boon EM, Jackson NM, Wightman MD et al (2003) Intercalative stacking: a critical feature of DNA charge-transport electrochemistry. *J Phys Chem B* 107:11805–11812. <https://doi.org/10.1021/jp030753i>
11. Rohs R, Sklenar H (2004) Methylene blue binding to DNA with alternating at base sequence: minor groove binding is favored over intercalation. *J Biomol Struct Dyn* 21:699–711. <https://doi.org/10.1080/07391102.2004.10506960>
12. Nejdil L, Kynický J, Brtnický M et al (2017) Amalgam electrode-based electrochemical detector for on-site direct determination of cadmium(II) and lead(II) from soils. *Sensors* 17:1835–1847. <https://doi.org/10.3390/s17081835>
13. Fischer J, Hajkova A, Pereira M et al (2016) Investigation of voltammetric behaviour of insecticide chlorpyrifos on a mercury meniscus modified silver solid amalgam electrode. *Electrochim Acta* 216:510–516. <https://doi.org/10.1016/j.electacta.2016.09.013>
14. Novakova K, Hrdlicka V, Navratil T et al (2016) Application of silver solid amalgam electrode for determination of formamide amitraz. *Monatsh Chem* 147:181–189. <https://doi.org/10.1007/s00706-015-1575-8>
15. Nováková K, Hrdlička V, Navrátil T et al (2015) Determination of 5-nitroindazole using silver solid amalgam electrode. *Monatsh Chem* 146:761–769. <https://doi.org/10.1007/s00706-014-1346-y>
16. Bandžuchová L, Šelešiovská R, Navrátil T, Chýlková J (2013) Silver solid amalgam electrode as a tool for monitoring the electrochemical reduction of hydroxocobalamin. *Electroanalysis* 25:213–222. <https://doi.org/10.1002/elan.201200365>
17. Mikkelsen O, Schroder KH (2003) Amalgam electrodes for electroanalysis. *Electroanalysis* 15:679–687. <https://doi.org/10.1002/elan.200390085>
18. Yosypchuk B, Fojta M, Barek J (2010) Amalgam electrodes as tool for study of environmental important compounds and for detection of DNA damages. *Int Conf Dev Energy Environ Econ Proc* 146–150
19. Yosypchuk B, Novotný L (2002) Electrodes of nontoxic solid amalgams for electrochemical measurements. *Electroanalysis* 14:1733–1738. <https://doi.org/10.1002/elan.200290018>
20. Yosypchuk B, Barek J (2009) Analytical applications of solid and paste amalgam electrodes. *Crit Rev Anal Chem* 39:189–203. <https://doi.org/10.1080/10408340903011838>
21. Vyskočil V, Daňhel A, Fischer J et al (2010) Silver amalgam electrodes — a look back at the last five years of their development and applications. *Sens Electroanal* 5:13–31
22. Lucca BG, Petroni JM, Ferreira VS (2018) Electrochemical study and voltammetric determination of sodium diethyldithiocarbamate using silver nanoparticles solid amalgam electrode. *Int J Environ Anal Chem* 99:397–408. <https://doi.org/10.1080/03067319.2018.1510918>
23. Barek J, Fischer J, Moreira JC, Wang J (2014) Voltammetric and amperometric determination of biologically active organic compounds using various types of silver amalgam electrodes. *Sens Electroanal* 8:35–47
24. Bobrowski A, Królicka A, Bobrowski R (2016) Renewable silver amalgam film electrodes in electrochemical stripping analysis — a review. *J Solid State Electrochem* 20:3217–3228. <https://doi.org/10.1007/s10008-016-3275-7>
25. Jusková P, Ostatná V, Paleček E, Foret F (2010) Fabrication and characterization of solid mercury. *Anal Chem* 82:2690–2695. <https://doi.org/10.1021/ac902333s>
26. Kuchariková K, Novotný L, Yosypchuk B, Fojta M (2004) Detecting DNA damage with a silver solid amalgam electrode. *Electroanalysis* 16:410–414. <https://doi.org/10.1002/elan.200302874>
27. Hasoň S, Dvořák J, Jelen F, Vetterl V (2002) Impedance analysis of DNA and DNA-drug interactions on thin mercury film electrodes. *Crit Rev Anal Chem* 32:167–179. <https://doi.org/10.1080/10408340290765515>
28. Krejčova Z, Barek J, Vyskočil V (2016) Voltammetric determination of fenitrothion and study of its interaction with DNA at a mercury meniscus modified silver solid amalgam electrode. *Monatsh Chem* 147:135–142. <https://doi.org/10.1007/s00706-015-1595-4>
29. Fadrná R, Yosypchuk B, Fojta M et al (2004) Voltammetric determination of adenine, guanine, and DNA using liquid mercury free polished silver solid amalgam electrode. *Anal Lett* 37:399–413. <https://doi.org/10.1081/Al-120028615>
30. Fadrná R, Cahová-Kuchariková K, Havran L et al (2005) Use of polished and mercury film-modified silver solid amalgam electrodes in electrochemical analysis of DNA. *Electroanalysis* 17:452–459. <https://doi.org/10.1002/elan.200403181>
31. Svitková V, Nemčeková K, Vyskočil V (2022) Application of silver solid amalgam electrodes in electrochemical detection of DNA damage. *Anal Bioanal Chem* 414:5435–5444. <https://doi.org/10.1007/s00216-022-03917-8>
32. Aruji Nicolai SH, Rodrigues PRP, Agostinho SML, Rubim JC (2002) Electrochemical and spectroelectrochemical (SERS) studies of the reduction of methylene blue on a silver electrode. *J Electroanal Chem* 527:103–111. [https://doi.org/10.1016/S0022-0728\(02\)00832-X](https://doi.org/10.1016/S0022-0728(02)00832-X)
33. Wopschall RH, Shain I (1967) Adsorption characteristics of the methylene blue system using stationary electrode polarography. *Anal Chem* 39:1527–1534. <https://doi.org/10.1021/ac50156a019>
34. Silva FB, Vieira SN, Goulart Filho LR, Boodts JFC, Brito-Madurro AG, Madurro JM (2008) Electrochemical investigation of oligonucleotide-DNA hybridization on poly(4-methoxyphenethylamine). *Int J Mol Sci* 9:1173–1188. <https://doi.org/10.3390/ijms9071173>
35. Piccardi G, Pergola F, Foresti ML, Guidelli R (1977) A detailed analysis of the polarographic behaviour of methylene blue in phosphate buffer on mercury. *J Electroanal Chem* 84:235–253. [https://doi.org/10.1016/S0022-0728\(77\)80375-6](https://doi.org/10.1016/S0022-0728(77)80375-6)
36. Komura T, Niu GY, Yamaguchi T, Asano M, Matsuda A (2004) Coupled electron-proton transport in electropolymerized methylene blue and the influence of its protonation level on the rate of electron exchange with  $\beta$ -nicotinamide adenine dinucleotide. *Electroanalysis* 16:1791–1800. <https://doi.org/10.1002/elan.200303029>
37. Vyskočil V, Blašková M, Hájková A et al (2012) Electrochemical DNA biosensors — useful diagnostic tools for the detection of damage to DNA caused by organic xenobiotics (a review). *Sens Electroanal* 7:141–162
38. Zhu L, Zhao R, Wang K et al (2008) Electrochemical behaviors of methylene blue on DNA modified electrode and its application to the detection of PCR product from NOS sequence. *Sensors* 8:5649–5660. <https://doi.org/10.3390/s8095649>
39. Li C, Chen X, Wang N, Zhang B (2017) An ultrasensitive and label-free electrochemical DNA biosensor for detection of DNase



- I activity. *RSC Adv* 7:21666–21670. <https://doi.org/10.1039/c7ra01995e>
40. Gu T, Hasebe Y (2004) Peroxidase and methylene blue-incorporated double stranded DNA–polyamine complex membrane for electrochemical sensing of hydrogen peroxide. *Anal Chim Acta* 525:191–198. <https://doi.org/10.1016/j.aca.2004.07.070>
  41. Gebala M, Stoica L, Neugebauer S, Schuhmann W (2009) Label-free detection of DNA hybridization in presence of intercalators using electrochemical impedance spectroscopy. *Electroanalysis* 21:325–331. <https://doi.org/10.1002/elan.200804388>
  42. Cesiulis H, Tsyntsaru N, Ramnavicius A, Ragoisha G (2016) The study of thin films by electrochemical impedance spectroscopy. In: Tiginyanu I, Topala P, Ursaki V (eds) *Nanostructured and thin films for multifunctional applications*. Springer, Switzerland, pp 3–42
  43. Al-Qasbi N, Hameed A, Khan AN et al (2018) Mercury meniscus on solid silver amalgam electrode as a sensitive electrochemical sensor for tetrachlorvinphos. *J Saudi Chem Soc* 22:496–507. <https://doi.org/10.1016/j.jscs.2016.07.005>
  44. Arias P, Ferreyra NF, Rivas GA, Bollo S (2009) Glassy carbon electrodes modified with CNT dispersed in chitosan: analytical applications for sensing DNA–methylene blue interaction. *J Electroanal Chem* 634:123–126. <https://doi.org/10.1016/j.jelechem.2009.07.022>
  45. Fojta M, Daňhel A, Havran L, Vyskočil V (2016) Recent progress in electrochemical sensors and assays for DNA damage and repair. *TrAC - Trends Anal Chem* 79:160–167. <https://doi.org/10.1016/j.trac.2015.11.018>

**Publisher's Note** Springer Nature remains neutral with regard to jurisdictional claims in published maps and institutional affiliations.

Springer Nature or its licensor holds exclusive rights to this article under a publishing agreement with the author(s) or other rightsholder(s); author self-archiving of the accepted manuscript version of this article is solely governed by the terms of such publishing agreement and applicable law.